DOI: 10.55415/deep-2023-0011.v1

Phenylethanoid Glycoside Verbascoside Ameliorates Podocyte Injury of Diabetic Kidney Disease via Regulating the NR4A1-LKB1-AMPK Signaling

Xinyun Chen [1], Min Shi [1], Letian Yang [1], Fan Guo [1], Yan Liang [2], Liang Ma [1,*], Ping Fu [1]

[1] Kidney Research Institute, Division of Nephrology, West China Hospital of Sichuan University, Chengdu 610041, China.

[2] Research Core Facility of West China Hospital, Chengdu 610041, China.

* To whom correspondence should be addressed: Liang Ma, Kidney Research Institute, West China Hospital of Sichuan University, Chengdu 610041, China. Email: Liang_m@scu.edu.cn (L Ma).

Running title: Verbascoside alleviates diabetic kidney disease

DOI: 10.55415/deep-2023-0011.v1

Highlights

1. Verbascoside alleviated blood glucose, proteinuria and pathological damages against DKD.

2. Verbascoside regulated inflammation, apoptosis and autophagy in podocytes of DKD.

3. Verbascoside reversed NR4A1-LKB1-AMPK signaling to exert therapeutic for DKD.

DOI: 10.55415/deep-2023-0011.v1

Abstract

Diabetic kidney disease (DKD) is one of the leading causes of end-stage renal disease. Verbascoside is a widespread phenylethanoid glycoside with potent anti-inflammatory, antioxidant and hypoglycemic properties. And this study aimed to explore the renoprotective effect of verbascoside against DKD with the underlying mechanism. After administration of verbascoside for four consecutive weeks, fast blood glucose, albumin-creatinine ratio and podocyte damage in diabetic mice were alleviated, especially at the dose of 150mg/kg/d. Moreover, inflammatory response, cell apoptosis and autophagy were improved dose-dependently in the kidneys of diabetic mice and high glucose-stimulated podocytes. Mechanistically, verbascoside reversed the elevated NR4A1 expression and suppressed LKB1 to inhibit AMPKα phosphorylation. Silencing NR4A1 could inhibit the LKB1 and phospho-AMPKα expression, and it could relieve stress response in injured podocytes. Collectively, our results indicated that verbascoside alleviated podocyte injury of DKD via regulating the NR4A1-LKB1-AMPK signaling.

Keywords: Verbascoside; Diabetic nephropathy; NR4A1; LKB1; AMPKα.

DOI: 10.55415/deep-2023-0011.v1

1. Introduction

Nowadays, the prevalence of diabetes has surged with lifestyle changes. According to the International Diabetes Federation (IDF), there were more than 537 million people with diabetes in 2021[1] (https://diabetesatlas.org). Patients with diabetes often suffer from multiple complications such as retinopathy, nephropathy, neuropathy, and cardiovascular diseases, which reduce both their quality of life and life expectancy[2]. And it is estimated that about 40% of patients with diabetes are complicated with diabetic kidney disease (DKD)[3].

DKD is one of the principal causes of chronic kidney disease (CKD) and end-stage renal disease (ESRD)[4]. However, the mechanisms of DKD are complex and poorly explored. Current studies indicated that DKD is a multifactorial disease whose pathogenesis includes glomerular hypertension, changes in renal hemodynamics, renal ischemia and hypoxia, upregulation of the renin-aldosterone system, etc[5]. Therefore, the treatment for DKD also relies on multiple interventions, including renin-angiotensin system (RAS) blockade, hypoglycemic drugs and other metabolic control[6, 7]. Besides, some large clinical studies have demonstrated effective drugs that could alleviate the progression of DKD. For example, the CREDENCE trial (the Canagliflozin and Renal Events in Diabetes with Established Nephropathy Clinical studies of Evaluation) found that SGLT2 inhibitors improved the prognosis of DKD and reduced the risk of kidney failure[8]. The FIDELIO-DKD trial (Finerenone in Reducing Kidney Failure and Disease Progression in Diabetic Kidney Disease) showed that Finerenone lowered the risks of CKD progression and cardiovascular

DOI: 10.55415/deep-2023-0011.v1

events compared with placebo[9]. Unfortunately, although these interventions could delay the progression of DKD, ESRD is still inevitable for some patients. Consequently, promising and novel treatments preventing DKD are still required.

Verbascoside (or acteoside, PubChem CID: 5281800) is a widespread phenylethanoid glycoside, which is distributed among more than 200 plant species from 23 plant families with different concentrations[10]. Verbascoside has been proven to possess wound-healing, neuroprotective, anti-inflammatory, antioxidant and anti-tumor properties[10, 11], and these properties displayed potential nephroprotective effects. Previous studies also indicated that drugs mainly containing verbascoside could reduce blood glucose and improve renal function in the experimental model of diabetic mice[12, 13]. However, the versatile role of verbascoside against DKD has not been well characterized, and the present study aimed to explore the therapeutic effect of verbascoside in DKD with the underlying mechanism.

2. Material and methods

2.1 Chemicals and reagents

Verbascoside was purchased from MedChem Express (HY-N0021). Antibodies to NR4A1 (25851-1-AP) and caspase-3 (66470-2-Ig) were purchased from Proteintech, US. Antibodies to LKB1 (sc-32245), podocin (sc-518088), and nephrin (sc-376522) were purchased from Santa Cruz, US. Antibodies to AMPKα (5831), pAMPKα(50081), cleaved caspase-3 (AF0120), caspase-3, Beclin-1 (3495), p62 (8025S), Atg5 (2630S) were obtained from Cell Signaling Technology, US. Anti-

DOI: 10.55415/deep-2023-0011.v1

CXCL10 (ab9807) was purchased from Abcam, US. Anti-LC3B (AF4650), Bcl-2 (AF6139), Bcl-xL (AF6414), Bax (AF0120) and anti-MCP-1 (DF7577) were purchased from Affinity Bioscience, US. Antibodies to β-actin (ET1701-80) and IL-6 (EM170414) were purchased from Hangzhou HuaAn Biotechnology, China.

2.2 Animal experiments

The animal experimental protocols were approved by the Ethics Committee for Experimental Research and Animal Care and Use Ethics Committee of Sichuan University (2020061A), and the animal care and experimental procedures were performed following The Guide for the Care and Use of Laboratory Animals from National Research Council (US) Committee. Male C57BLKS/J db/db and db/+ mice (6 weeks old) were purchased from GemPharmatech biotechnology company (Nanjing, China). The mice were housed in a temperature-controlled room (23 ± 2 °C) under a 12-h light/dark cycle with free access to food and water. After 2 weeks of the adaptation period, the C57BLKS/J db/db mice were randomly divided into three groups, diabetic group (n=6), low-dose treatment group (75 mg/kg, n=6) and high-dose treatment group (150 mg/kg, n=6). The db/+ mice were divided into the control group (n=12). Verbascoside was dissolved in 10% DMSO, 40% PEG300, 5% Tween-80 and 45% normal saline, and further diluted in normal saline before gavaging to db/db mice. Equal volumes of normal saline were administered once daily to db/+ control group and db/db model group. All mice were sacrificed after 4 weeks of treatment.

DOI: 10.55415/deep-2023-0011.v1

2.3 Biochemical analyses

The 12 h fasting blood glucose levels in mice were collected from the tail vein every week and the level of urine albumin was determined using an automatic biochemical analyzer (BS-240, Mindray, Shenzhen, China).

2.4 Cell culture and treatments

Mouse podocyte clone 5 (MPC5, ATCC® CCL-171™, Beijing bnbio Co. Ltd, Beijing, China) cells were propagated at 33°C and treated with interferon (IFN-γ; 10 U/mL). Next, cells were differentiated without IFN-γ at 37°C for 14 days. For further study, MPC5 cells were cultured in RPMI-1640 (SH30809.01B, HyClone, Beijing, China), with 10% FBS (SH30084.03, Hyclone, Beijing, China), 0.5% penicillin and streptomycin (SV30010, HyClone, Beijing, China), under 37°C and 5% CO_2. The Cells were serum-starved in the medium containing 0.5% serum for 24 h and then treated with high glucose (30 mM glucose) or mannitol (24.5 mM mannitol + 5.5 mM glucose) with or without incubation of verbascoside for 24 h.

2.5 Cell viability assay

To explore the potential effects of verbascoside on cell viability, a Cell Counting Kit-8 assay (CCK-8, Dalian, China) was employed. In brief, MPC5 cells (5000-10000 cells/well) were seeded into 96-well plates for 24 h and later incubated with verbascoside at various concentrations (25, 50, 75, 100, 200, 300, 400 μM). Then, the culture media of each well was replaced with 10 μL CCK-8 solutions, and the cells were incubated without lighting at 37°C for 1 h. At last, the absorbance of the solution

DOI: 10.55415/deep-2023-0011.v1

in each well was detected at 450 nm wavelength by a microplate reader (Synergy Mx, Biotek, Winooski, VT, USA).

2.6 Renal histological examination

Kidney tissues were fixed in 10 % neutral buffered formalin, embedded in paraffin, and sectioned at 4 μm thickness. After deparaffinization and rehydration, kidney sections were respectively stained with periodic acid-Schiff (PAS), Weigert's iron hematoxylin (MASSON) or hematoxylin and eosin (HE). The sections were viewed by light microscopy at magnifications of ×200 or ×400. Finally, the mesangial expansion index of renal tissue was evaluated from 10 randomly selected fields.

2.7 Transmission electron microscopy

Kidney tissues were fixed in cold 2.5% glutaraldehyde for 2 h at 4 °C and then treated with standard procedures, including dehydration, osmosis, embedding, sectioning, and staining, and finally visualized on a Hitachi microscope (H-7650, Calgary, AB, Japan) at ×8000, ×12,000, and ×20,000 magnifications.

2.8 Quantitative Real-Time PCR analysis

Renal tissue and total cellular RNA were extracted by total RNA isolation kit (Foregene, Chengdu, China) and its concentration and purity were determined by ScanDrop 100 (Analytik Jena, Thuringia, Germany). Then, reverse transcription was performed with HiScript III SuperMix (Vazyme, Nanjing, China). The iTaqTM Universal SYBR Green Supermix (Bio-Rad, Hercules, CA, USA) was employed for quantitative real-time PCR in a PCR system (CFX Connect; Bio-Rad). Primer

DOI: 10.55415/deep-2023-0011.v1

sequences were listed in Supplementary Table 1. The mRNA levels were normalized to β-actin and calculated using the comparative cycle threshold ($2^{-\Delta\Delta Ct}$) method.

2.9 Immunohistochemistry

After fixation in 10 % phosphate-buffered formalin overnight, the fixed kidneys were dehydrated through a graded series of ethanol, embedded in paraffin, sectioned (4 μm), and mounted on glass slides. The slides were blocked with 2.5 % normal goat serum and incubated with primary antibodies at 4℃. The slides were washed thrice in PBS, and VECTASTAIN ABC Kit (Vector, Burlingame, CA, United States) was used for staining following the manufacturer's instructions. The sections were counterstained with hematoxylin. Images were captured using an AxioCamHRc digital camera (Carl Zeiss).

2.10 Immunofluorescence staining

OCT-embedded kidney sections (4 μm) were incubated with phosphate-buffered saline (PBS) containing 5% horse serum for 1 h at room temperature to block non-specific binding sites. Then the specimens were incubated with primary antibody anti-Nephin (1:200) or anti-Podocin (1:200) in a humidified chamber overnight at 4°C. After washing, the secondary antibody (1:500) was used for 1 h. The samples were washed again. Then, the samples were stained with DAPI (1:500). Finally, the samples were sealed with coverslips. Images were acquired by an AxioCamHRc digital camera (Carl Zeiss, Jena, Germany) at magnifications of ×400 with ZEN 2012 microscopy software (blue edition).

DOI: 10.55415/deep-2023-0011.v1

2.11 Western blot analysis

Western blot analysis was performed as described earlier[14]. Densitometry analysis was performed using Image J 6.0 software (National Institutes of Health, Bethesda, MD, United States).

2.12 RNA-Seq transcriptomic assay

Total RNA from kidneys of each treatment group (n = 3) was isolated with the Trizol reagent (Invitrogen, Carlsbad, CA, USA). Library constriction and sequencing were performed by LC-BIO Biotech Ltd. (Hangzhou, China). The libraries were sequenced on an Illumina NovaSeqTM 6000 platform and 2×150-bp paired-end reads were generated. Further bioinformatic analysis was performed using the OmicStudio tools at https://www.omicstudio.cn/tool.

2.13 Cell siRNA transfection

Transient transfections of the MPC5-1 cells with siRNAs were conducted with transfection reagent (riboFECTTM CP transfection kit (166T); RiboBio, Guangzhou, China) according to the manufacturer's instructions[15, 16]. The sequences of NR4A1 siRNA and negative control (NC) siRNA were as follows: NR4A1 siRNA, sense 5'-GCCCUGUAUUCAAGCUCAATT-3' and antisense 5'-UUGAGCUUGAAUACAGGGCTT-3'; NC siRNA sense 5'-UUCUCCGAACGUGUCACGUTT-3' and antisense 5'-ACGUGACACGUUCGGAGAATT-3' (GenePharma, Shanghai, China). MPC5 cells were seeded in six-well plates and transfected with a final concentration of 100 nM

DOI: 10.55415/deep-2023-0011.v1

siRNA using riboFECTTM CP reagent (RiboBio, Guangzhou, China) in RPMI-1640 medium containing 0.5% fetal bovine serum (SH30084.03, HyClone, Beijing, China) without penicillin-streptomycin for 24 h.

2.14 Molecular docking

The three-dimensional structure of verbascoside was obtained from PubChem (https://pubchem.ncbi.nlm.nih.gov/). The crystal structure of NR4A1 was downloaded from the Protein Data Bank (PDB, https://www. rcsb.org/). The AutoDockTools (version 1.5.6, http://autodock.scripps. edu/) were used to convert the downloaded verbascoside and NR4A1 to the pdbqt format. Molecular docking was performed with the AutoDock Vina (version 1.12, http://vina.scripps.edu/). The docking pose of verbascoside and NR4A1 was visualized with the PyMOL software (version 2.2, https://pymol.org/2/).

2.15 Statistical analysis

All experiments were performed in triplicate unless otherwise stated. Data are presented as mean ± SD. Statistical differences between the two groups were performed by two-tailed Student's t test (for parametric data) or Mann-Whitney U test (for non-parametric data). Comparisons between multiple groups were analyzed with one-way ANOVA (for one experimental parameter) or two-way ANOVA (for two experimental parameters) followed by Tukey's multiple comparisons test using GraphPad Prism 9.0.0 (GraphPad Software, San Diego, CA, USA). $P < 0.05$ was considered statistically significant.

DOI: 10.55415/deep-2023-0011.v1

3. Results

3.1 Verbascoside improved blood glucose, albuminuria, and renal histopathologic injury in diabetic mice

The chemical structure of verbascoside is shown in Fig. 1a. To evaluate whether verbascoside could protect against DKD, we treated 8-week-old db/db mice with verbascoside (at the dose of 75mg/kg or 150mg/kg) for 4 weeks. As presented in Figure 1b, verbascoside at a dose of 150 mg/kg/d (db-150VB) remarkably lowered the level of fast blood glucose (FBG) and albumin creatinine ratio (ACR) than those of db/db mice ($P < 0.05$). Besides, the 150 mg/kg group (db-150VB) also alleviated kidney pathological damage characterized by mesangial matrix expansion and glomerulosclerosis compared to diabetic mice (Fig. 1c and e). In contrast, the 75mg/kg group (db-75VB) had no apparent therapeutic effect.

Furthermore, as shown by the results of immunofluorescence staining and electron microscopy, verbascoside ameliorated podocyte injury (Fig. 1d and g). Nephrin and podocin are transmembrane proteins of podocytes, and their expression levels could indicate the degree of podocyte injury. The immunofluorescence staining showed the decreased expression of nephrin and podocin in db/db mice. At the same time, verbascoside administration restored the decrease phenomenon (Fig. 1d). Consistently, transmission electron microscopy analysis revealed that verbascoside at 150 mg/kg doses (db-150VB) alleviated foot process fusion, glomerular basement membrane thickness and mesangial cell proliferation (Fig. 1f and g). All these results indicated that verbascoside could protect against DKD.

DOI: 10.55415/deep-2023-0011.v1

3.2 Verbascoside suppressed cell stress responses in kidneys of diabetic mice and high-glucose triggered MPC5 podocytes

Accumulating evidence indicated that dysregulated inflammation, apoptosis, and autophagy are vital mechanisms in DKD[17-21]. Firstly, we employed q-PCR and western blot to detect the expression of pro‐inflammatory cytokines and chemokines in kidneys. As expected, both mRNA and protein levels of IL-6, CXCL10 and MCP-1 in kidney tissues were increased in db/db mice compared with db/+ mice. At the same time, verbascoside effectively reduced the corresponding expression, especially the dose of 150mg/kg/d group (Fig. 2a and b). Next, western blot results implicated the level of apoptosis increased in db/db mice compared with db/+ mice, which showed a decreased trend of Bcl-2 and Bcl-xL and an increasing trend of Bax and cleaved caspase-3 ($P< 0.05$). And verbascoside treatment increased the protein levels of Bcl-2 and Bcl-xL, and decreased the protein levels of cleaved caspase-3 and Bax , especially at the dose of 150mg/kg (Fig. 2d). Consistently, verbascoside reduced mRNA level of Bax, and increased mRNA levels of Bcl-2 and Bcl-xL (Fig. 2c). Additionally, verbascoside also promoted the levels of autophagy in db/db mice. Western blot analysis exhibited that verbascoside increased the Atg5, LC3-II, and Beclin-1 levels, which were down-regulated in the kidneys of db/db mice. Furthermore, the kidney level of p62/SQSTM1 protein was also decreased by verbascoside treatment (Fig. 2i and j).

Then, we employed CCK-8 assay to examine the cytotoxic effect of verbascoside (0-400 μM) in murine podocytes (MPC5 cells), and we found that cell viability was

DOI: 10.55415/deep-2023-0011.v1

inhibited at the dose of 200 μM (Supplementary Figure 1). Accordingly, three therapeutic concentrations (25 μM, 50 μM and 100 μM) were selected for the follow-up experiments, and we cultured MPC5 cells in high-glucose media (30 mM) for 24 h. The results revealed that high-glucose (HG) stimulation increased the pre-transcriptional and post-transcriptional levels of IL-6, CXCL10 and MCP-1 compared with the mannitol control group (MA). Verbascoside reversed the elevated expression of these pro inflammatory cytokines and chemokines, and the dose of 100 μM (100VB) was the most significant (Fig. 2e and f). Consistent with the results in vivo, apoptosis was raised by HG stimulation and alleviated by verbascoside. The expression of pro-apoptotic markers (cleaved caspase-3 and Bax) (Fig. 2g and h) as well as apoptotic rate by flow cytometry (Supplementary Figure 2) was significantly increased by HG stimulation and further decreased by verbascoside treatment ($P < 0.05$). In addition, verbascoside increased the expression of anti-apoptotic markers (Bcl-2 and Bcl-xL) that were reduced by high glucose (Fig. 2g and h). Furthermore, western blot results showed verbascoside increased protein levels of Atg5, LC3-II, and Beclin-1, and decreased protein levels of p62, compared with the HG group (Fig. 2j).

3.3 Predicting the target of verbascoside in the kidneys of diabetic mice

To reveal the mechanism of verbascoside in db/db mice, the RNA-seq transcriptomic analysis was employed. And significant verbascoside-regulated genes were illustrated by the heatmap in Figure 3a. Synaptopodin, a podocyte injury marker,

DOI: 10.55415/deep-2023-0011.v1

was downregulated in the kidneys of db/db mice and was upregulated in VB-150 group. This is consistent with our previous findings that verbascoside protected against podocyte injury. And genes related to inflammation (IL-1β, CXCL10), metabolism (Pparg) and cell cycle (Ccnb1, Mcm5, Bub1b and Espl1) were also detected to change among groups. Additionally, we found the transcription factor NR4A1, whose expression was markedly upregulated in the kidneys of db/db mice compared to db/+ mice, while verbascoside reversed the upregulation.

Furthermore, KEGG analysis presented that the AMPK signaling pathway, PPAR signaling pathway, fatty acid degradation and other metabolic pathways were involved (Figure 3b). This suggested that verbascoside may protect the injured kidneys by affecting metabolic pathways. Notably, AMPK pathways, which are responsible for regulating cell metabolism, played vital roles in DKD.

To further reveal the mechanism, molecular docking was performed. Verbascoside exhibited good affinity with NR4A1 protein, and verbascoside had a compact binding pattern with NR4A1 protein active pocket by forming hydrogen bonds with the amino acid residues GLN240, TYR244, ARG241, GLY65, SER222, HLS63, RPO62, LEU142, ASP153, ALA145, ARG241, TYR244 (Figure 3c). So, we hypothesized that verbascoside played a protective role in DKD by targeting NR4A1.

Previous studies have suggested that NR4A1 could regulate the phosphorylation of AMPKα[22, 23]. Given that NR4A1 was reported to bind LKB1 and then inhibited the activation of AMPKα[22, 23], we speculated that verbascoside alleviated DKD via NR4A1/LKB1/AMPK pathway. Further, we identified that NR4A1 expression was

DOI: 10.55415/deep-2023-0011.v1

increased in the kidneys of db/db mice compared with db/+. Besides, NR4A1 expression was reduced after verbascoside administration (Figure 3d, e, f and j). The high-glucose stimulation also could raise NR4A1 expression in podocytes, while verbascoside lowered NR4A1 expression (Figure 3g, h and i).

3.4 Verbascoside regulated NR4A1/LKB1/AMPK pathway in kidneys of diabetic mice and high-glucose triggered podocytes

To verify the hypothesis, we analyzed the expression of LKB1 and phospho-AMPKα in the kidneys of mice. We found that both LKB1 and phospho-AMPKα of db/db mice were downregulated compared with db/+ mice. And verbascoside reversed the downregulation (Figure 4a-b). Consistently, verbascoside also increased the expression of LKB1 and phospho-AMPKα in HG-stimulated MPC5 cells (Figure 4c-d). Next, NR4A1 knockdown by siRNA technology (Supplementary Figure 3a-b) promoted the expression of LKB1 and phospho-AMPKα to a similar extent as verbascoside treatment (Figure 4e-f).

3.5 Inhibition of NR4A1 improved cell stress in high-glucose-triggered podocytes

As delineated in Figure 5, NR4A1 knockdown attenuated HG-stimulated inflammation as evidenced by reduced pro-inflammatory cytokines and chemokine (IL-6, MCP-1 and CXCL10) (Figure 5 a, d, e and f). In addition, NR4A1 knockdown reduced apoptosis stimulated by high glucose. Silencing NR4A1 triggered a decrease of pro-apoptotic markers (cleaved caspase-3 and Bax) (Figure 5b and i) and apoptotic rate by flow cytometry (Supplementary Figure 4). Silencing NR4A1 caused an

DOI: 10.55415/deep-2023-0011.v1

increase in anti-apoptotic markers (Bcl-2 and Bcl-xL) (Figure 5b, g and h). Besides, NR4A1 knockdown promoted autophagy, as evidenced by decreased expression of p62, and increased autophagy-related protein (Atg5, LC3-II, and Beclin-1) (Figure 5c). All in all, the results indicated that knockdown NR4A1 protected podocyte injury against high-glucose stimulation by inhibiting inflammation and apoptosis and improving autophagy.

4. Discussion

In the present study, we explored the nephroprotective role of verbascoside in DKD. By treating db/db mice with verbascoside for 4 consecutive weeks, proteinuria and pathological damages were significantly relieved. Moreover, the disordered cell stresses (increased inflammatory response and apoptosis, as well as autophagy dysfunction) were alleviated after verbascoside administration in a dose-dependent manner. Mechanistically, verbascoside downregulated the expression of NR4A1, and further upregulated the expression of LKB1 and phospho-AMPKα. Notably, NR4A1 knockdown in podocytes could also promote the expression of LKB1 and phospho-AMPKα. These observations support the therapeutic effect of verbascoside against DKD.

Previous studies reported that verbascoside or drugs containing verbascoside could reduce blood glucose, and it is consistent with the results of our study. For example, *Cistanche tubulosa*, whose main components include verbascoside, could significantly inhibit the increase of fasting blood glucose and improve insulin

DOI: 10.55415/deep-2023-0011.v1

resistance in db/db mice and STZ-induced diabetic rats [12, 24]. In addition, verbascoside alleviated endoplasmic reticulum stress in islet β cells[25]. And verbascoside improved the anti-cytotoxicity of high glucose in gingival cells[26]. Verbascoside also promoted bone formation in osteocytes of STZ-induced diabetic rats[26]. All these results indicate the potential nephroprotective efficiency of verbascoside in diabetic complications.

NR4A1 is the possible target of verbascoside on DKD after we combine the results of transcriptomics and molecular docking. NR4A1, a member of the nuclear orphan receptor superfamily (NR4A), regulates various cellular activities, widely participates in cell metabolism, apoptosis, inflammation, and other biological events, and is closely related to a variety of metabolic diseases[27]. NR4A1 is an early response gene, and its changes are rapidly induced by a variety of substances, such as cytokines, glucose, fatty acids, lipopolysaccharides and other small molecular compounds[28-31]. Hyperfunction or dysfunction of NR4A1 could affect metabolic processes in primary metabolic tissues, like influencing glucose metabolism and lipid metabolism in the liver, skeletal muscle, pancreatic tissue, and adipose tissue [32-34]. Notably, NR4A1 is also an essential regulator for diabetes and its complications. Previous studies showed that the expression of NR4A1 was increased in both type 1 and type 2 diabetic animal models[34, 35], which is in line with our results. Overexpression of NR4A1 by adenovirus induced the expression of gluconeogenesis-related genes[34]. Then, glucose production and blood glucose level were promoted [34]. Consistently, NR4A1 agonists like CSN-B (Octaketide cytosporone B) had a similar effect on elevating hepatic glucose production and blood glucose[36]. In addition, the cAMP axis induced hepatic

DOI: 10.55415/deep-2023-0011.v1

NR4A1 expression in response to glucagon and fasting[34]. However, the biological function of NR4A1 is complex and poorly understood. For example, knockout of NR4A1 could lead to systemic inflammation in aged mice[37], aggravated colitis in mice[38] and promote the differentiation of macrophages into a pro-inflammatory M1 phenotype[39]. However, these results were contrary to our results that NR4A1 knockout mitigated inflammation of podocytes. There are also similar results with us that reported the upregulation of NR4A1 promoted inflammation like NF-κB pathway[31], and knockdown of NR4A1 inhibited inflammation-related molecules like TNF-α and IL-6[22]. It seems that the results should be explained in specific experimental conditions like different disease and stimulation conditions since the sophisticated function of NR4A1. Considerably more work will need to be done to explore the role of NR4A1 in the future.

In conclusion, our study illustrated the therapeutic effect of phenylethanoid glycoside verbascoside in DKD. Mechanistically, verbascoside downregulated NR4A1 and further influenced the LKB1/AMPK pathway. Our results highlighted that verbascoside might be a potential approach for the therapy of DKD.

Acknowledgments

This study was supported by the Science/Technology Project of Sichuan province [2021YFQ0027 and 2022YFS0589].

Conflict of interest

The authors declare that there is no conflict of interest regarding the publication of

DOI: 10.55415/deep-2023-0011.v1

this paper.

DOI: 10.55415/deep-2023-0011.v1

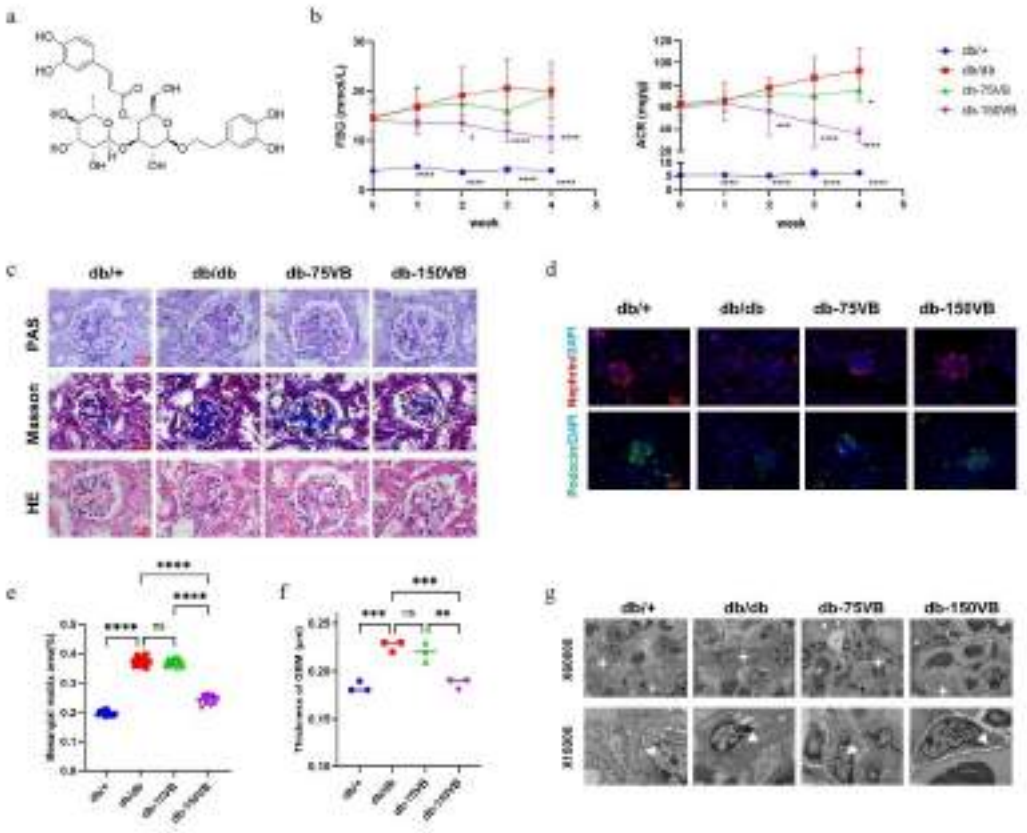

Figure 1 Verbascoside ameliorated kidney injury in db/db mice. (a) Chemical structure of verbascoside. (b) Fast blood glucose (FBG) and albumin creatinine ratio (ACR). vs db/db group(n = 6). (c) Representative pathological staining micrographs (PAS, Masson and HE staining, ×1000, scale bar = 10 μm). (d) Representative immunofluorescence staining micrographs of nephrin (red) and podocin (green) in the renal cortex (×400, scale bar = 20 μm). (e) Quantification of the fraction of mesangial area. (f) Measurements of glomerular basement membrane (GBM) thickness. (g) Transmission electron microscopy showed thickening of the basement membrane, fusion of podocyte foot process (the arrows indicate), and hyperplasia of mesangial cells (the stars indicate) in db/db mice, while these pathological lesions were alleviated after verbascoside treatment. *P < 0.05, ** P < 0.01, ***P < 0.001, **** P < 0.0001.

DOI: 10.55415/deep-2023-0011.v1

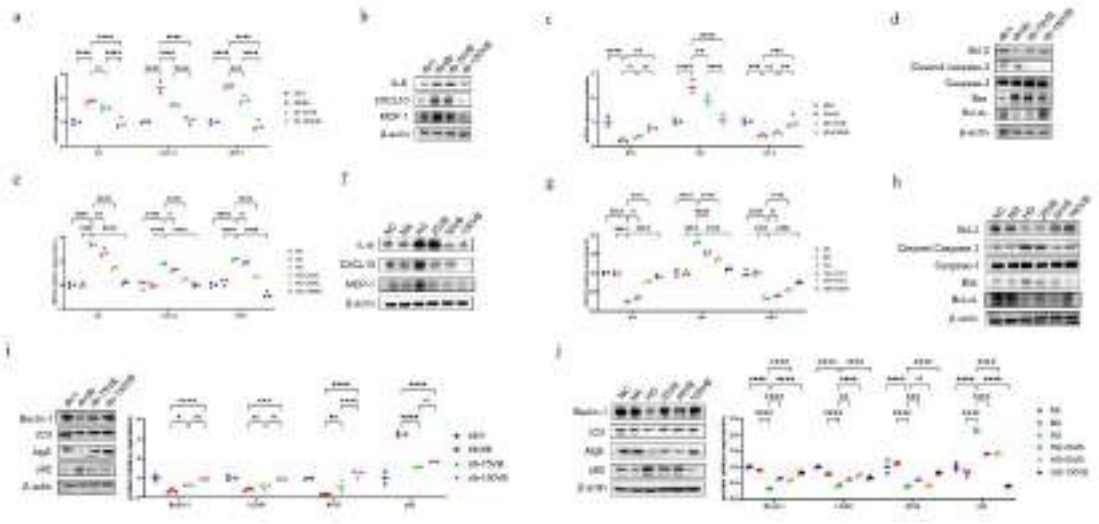

Figure 2 Verbascoside ameliorated cell stress responses in vitro and vivo. The mRNA levels of IL-6, CXCL10, and MCP-1 in renal tissues (a) and MPC5 cells (e) were analyzed by RT-PCR. The protein levels of IL-6, CXCL10, and MCP-1 in renal tissues (b) and MPC5 cells (f) were detected by western blot. The mRNA levels of Bcl-2, Bax and Bcl-xL in renal tissues (c) and MPC5 cells (g) were analyzed by RT-PCR. The protein levels of Bcl-2, cleaved caspase-3/caspase-3, Bax and Bcl-xL in renal tissues (d) and MPC5 cells (h) were detected by western blot. Western blot showed the protein expression levels of Beclin-1, LC3-II, Atg5 and p62 of renal tissues (i) and MPC5 cells (j). All data are represented as the mean ± SD (n =3). *$P < 0.05$, ** $P < 0.01$, ***$P < 0.001$, **** $P < 0.0001$.

DOI: 10.55415/deep-2023-0011.v1

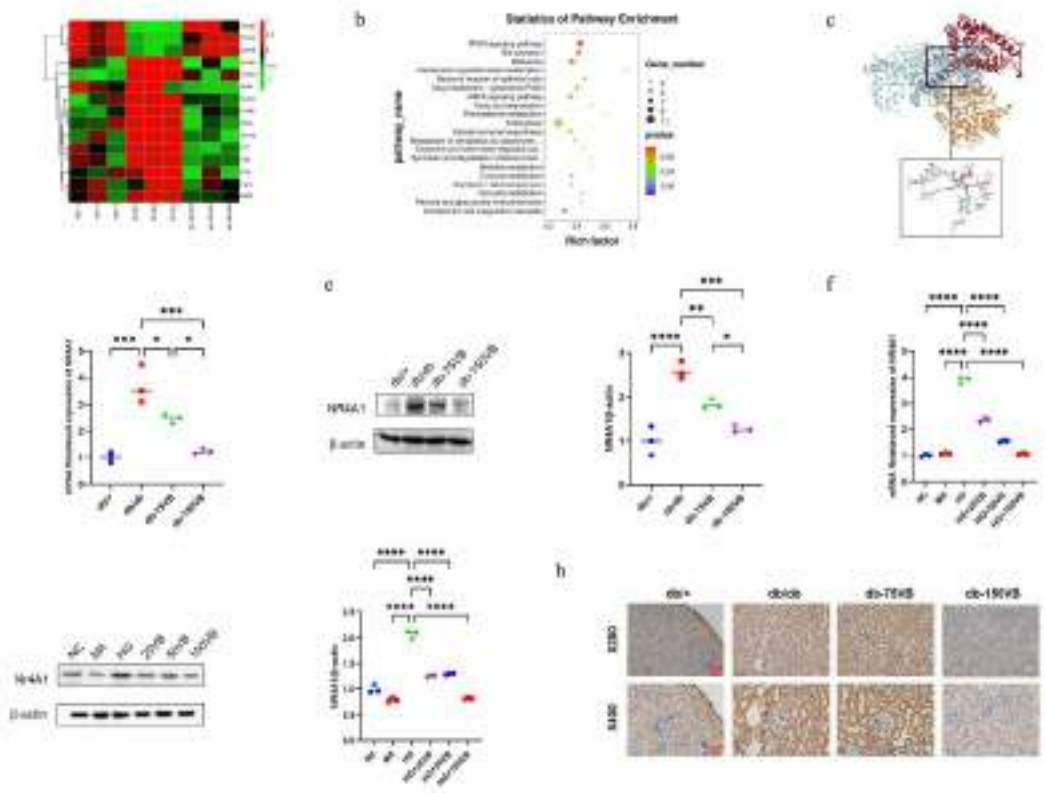

Figure 3 Verbascoside ameliorated DKD by regulating the expression of NR4A1. (a) Representative heatmap of differentially expressed genes in kidneys. (b) KEGG pathways analysis of genes regulated by verbascoside. (c) Molecular docking of verbascoside binding to NR4A1. The mRNA (d) and protein (e) levels of NR4A1 in mice renal tissues were shown. The mRNA (f) and protein (g) levels of NR4A1 in MPC5 cells were detected. (h) Representative images of immunohistochemistry staining for NR4A1in kidneys of diabetic mice. All data are represented as the mean ± SD (n = 3).*P < 0.05, ** P < 0.01, ***P < 0.001, **** P < 0.0001.

DOI: 10.55415/deep-2023-0011.v1

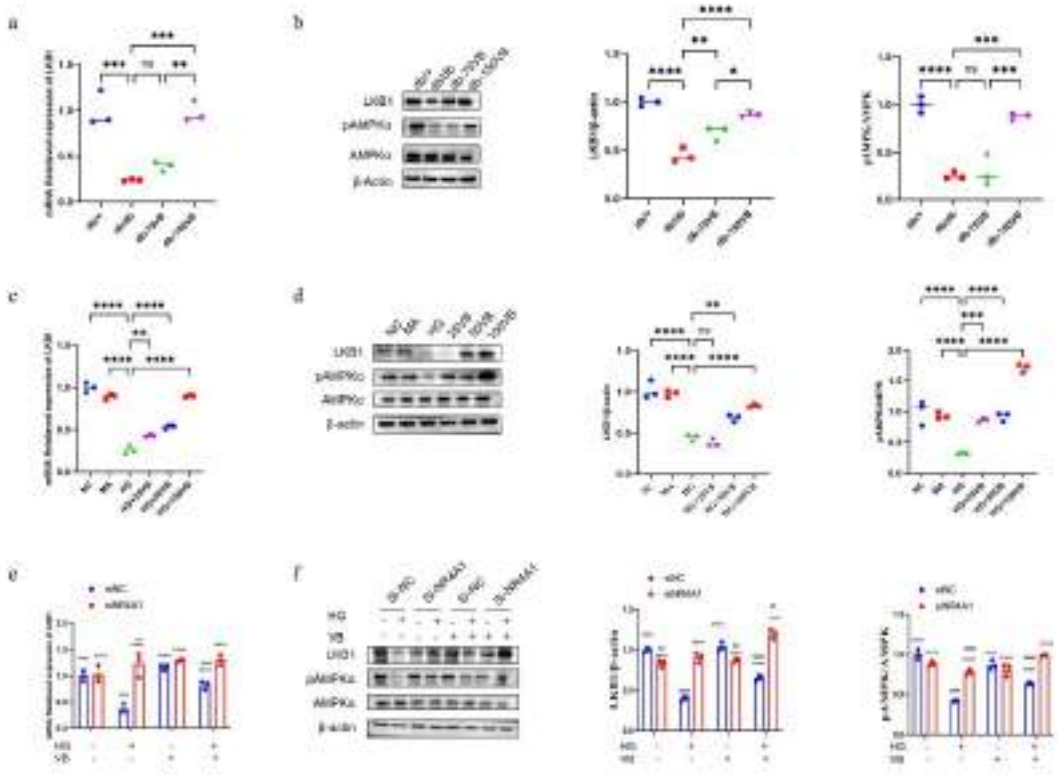

Figure 4 Effects of verbascoside on NR4A1/LKB1/AMPK signaling pathway in vitro and vivo. The mRNA levels of LKB1in renal tissues (a) and HG-stimulated MPC5 cells (c) were detected by RT-PCR. The protein levels of LKB1, pAMPKα and AMPKα in renal tissues (b) and HG-stimulated MPC5 cells (d) were detected by western blot. MPC5 cells were transfected with negative control (NC) siRNA or NR4A1 siRNA for 24 h with or without the treatment of HG or verbascoside. Then, the mRNA level of LKB1 (e) and protein levels of LKB1, pAMPKα and AMPKα (f) was evaluated. All data are represented as the mean ± SD (n =3). *$P < 0.05$, ** $P < 0.01$, ***$P < 0.001$, **** $P < 0.0001$ compared with the HG group. #$P < 0.05$, ## $P < 0.01$, ### $P < 0.001$, #### $P < 0.0001$ compared with the control group.

DOI: 10.55415/deep-2023-0011.v1

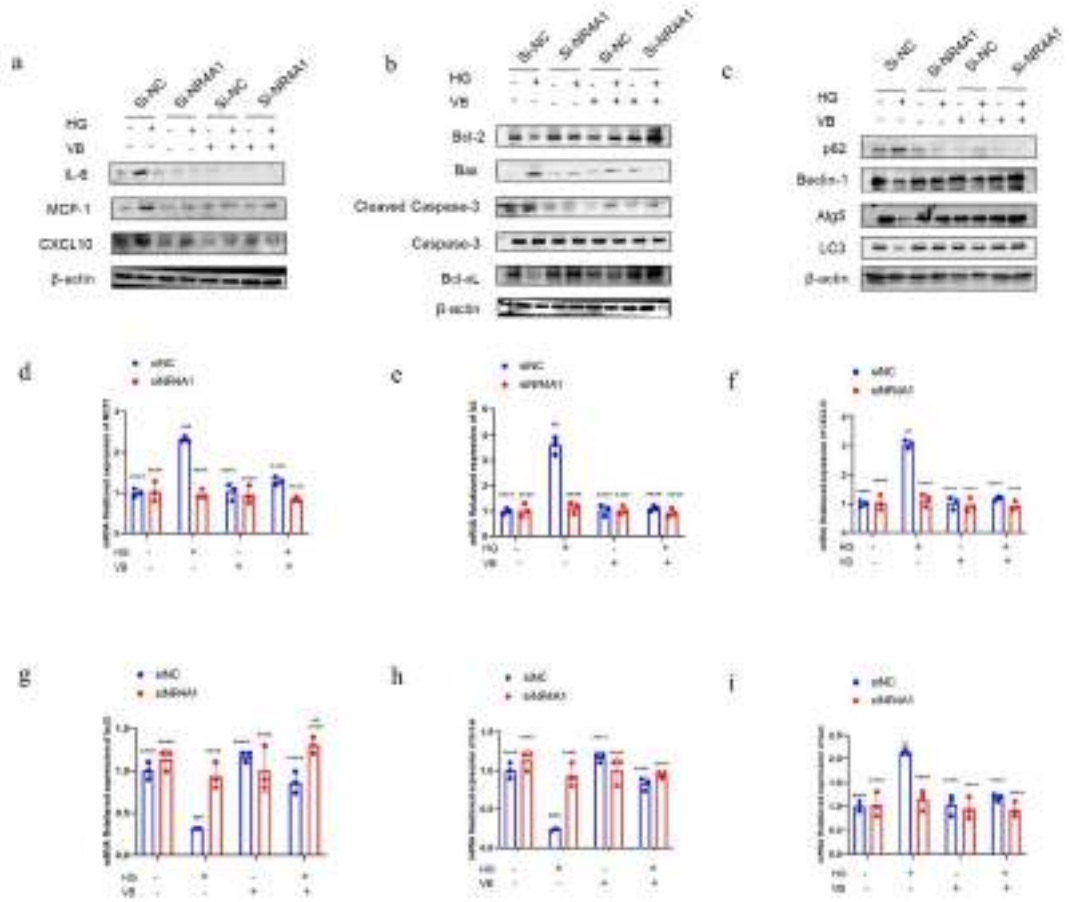

Figure 5 NR4A1 knockdown alleviated cell stress responses in high-glucose-triggered podocytes. MPC5 cells were transfected with negative control (NC) siRNA or NR4A1 siRNA for 24 h with or without the treatment of HG or verbascoside. Then, the protein (a) and mRNA (d-f) levels of IL-6, CXCL10, and MCP-1 were analyzed. (b) The protein levels of Bcl-2, cleaved caspase-3/caspase-3, Bax and Bcl-xL were detected by western blot. (g-i) The mRNA levels of Bcl-2, Bax and Bcl-xL were analyzed by RT-PCR. (c) Western blot showed the protein expression levels of Beclin-1, LC3-II, Atg5 and p62. All data are represented as the mean ± SD (n =3). *$P < 0.05$, ** $P < 0.01$, ***$P < 0.001$, **** $P < 0.0001$ compared with the HG group. #$P < 0.05$, ## $P < 0.01$, ### $P < 0.001$, #### $P < 0.0001$ compared with the control group.

DOI: 10.55415/deep-2023-0011.v1

References

1. K. Ogurtsova, L. Guariguata, N.C. Barengo, P.L. Ruiz, J.W. Sacre, S. Karuranga, H. Sun, E.J. Boyko, D.J. Magliano. IDF diabetes Atlas: Global estimates of undiagnosed diabetes in adults for 2021. ***Diabetes research and clinical practice***. 2022, 183: 109118. https://doi.org/10.1016/j.diabres.2021.109118

2. Y. Zheng, S.H. Ley, F.B. Hu. Global aetiology and epidemiology of type 2 diabetes mellitus and its complications. ***Nature reviews. Endocrinology***. 2018, 14: 88-98. https://doi.org/10.1038/nrendo.2017.151

3. S.M. Doshi, A.N. Friedman. Diagnosis and Management of Type 2 Diabetic Kidney Disease. ***Clinical journal of the American Society of Nephrology : CJASN***. 2017, 12: 1366-1373. https://doi.org/10.2215/cjn.11111016

4. K. Reidy, H.M. Kang, T. Hostetter, K. Susztak. Molecular mechanisms of diabetic kidney disease. ***The Journal of clinical investigation***. 2014, 124: 2333-2340. https://doi.org/10.1172/jci72271

5. M. Brownlee. Biochemistry and molecular cell biology of diabetic complications. ***Nature***. 2001, 414: 813-820. https://doi.org/10.1038/414813a

6. B. Fernandez-Fernandez, A. Ortiz, C. Gomez-Guerrero, J. Egido. Therapeutic approaches to diabetic nephropathy--beyond the RAS. ***Nature reviews. Nephrology***. 2014, 10: 325-346. https://doi.org/10.1038/nrneph.2014.74

7. Q. Yuan, B. Tang, C. Zhang. Signaling pathways of chronic kidney diseases, implications for therapeutics. ***Signal transduction and targeted therapy***. 2022, 7: 182. https://doi.org/10.1038/s41392-022-01036-5

8. V. Perkovic, M.J. Jardine, B. Neal, S. Bompoint, H.J.L. Heerspink, D.M. Charytan, R. Edwards, R. Agarwal, G. Bakris, S. Bull, C.P. Cannon, G. Capuano, P.L. Chu, D. de Zeeuw, T. Greene, A. Levin, C. Pollock, D.C. Wheeler, Y. Yavin, H. Zhang, B. Zinman, G. Meininger, B.M. Brenner, K.W. Mahaffey. Canagliflozin and Renal Outcomes in Type 2 Diabetes and Nephropathy. ***The New England journal of medicine***. 2019, 380: 2295-2306. https://doi.org/10.1056/NEJMoa1811744

9. G.L. Bakris, R. Agarwal, S.D. Anker, B. Pitt, L.M. Ruilope, P. Rossing, P. Kolkhof,

C. Nowack, P. Schloemer, A. Joseph, G. Filippatos. Effect of Finerenone on Chronic Kidney Disease Outcomes in Type 2 Diabetes. ***The New England journal of medicine***. 2020, 383: 2219-2229. https://doi.org/10.1056/NEJMoa2025845

10. K. Alipieva, L. Korkina, I.E. Orhan, M.I. Georgiev. Verbascoside--a review of its occurrence, (bio)synthesis and pharmacological significance. ***Biotechnology advances***. 2014, 32: 1065-1076. https://doi.org/10.1016/j.biotechadv.2014.07.001

11. Y. Xiao, Q. Ren, L. Wu. The pharmacokinetic property and pharmacological activity of acteoside: A review. ***Biomedicine & pharmacotherapy = Biomedecine & pharmacotherapie***. 2022, 153: 113296. https://doi.org/10.1016/j.biopha.2022.113296

12. W.T. Xiong, L. Gu, C. Wang, H.X. Sun, X. Liu. Anti-hyperglycemic and hypolipidemic effects of Cistanche tubulosa in type 2 diabetic db/db mice. ***Journal of ethnopharmacology***. 2013, 150: 935-945. https://doi.org/10.1016/j.jep.2013.09.027

13. X. Dai, S. Su, H. Cai, D. Wei, H. Yan, T. Zheng, Z. Zhu, E.X. Shang, S. Guo, D. Qian, J.A. Duan. Protective Effects of Total Glycoside From Rehmannia glutinosa Leaves on Diabetic Nephropathy Rats via Regulating the Metabolic Profiling and Modulating the TGF-β1 and Wnt/β-Catenin Signaling Pathway. ***Frontiers in pharmacology***. 2018, 9: 1012. https://doi.org/10.3389/fphar.2018.01012

14. T.T. Wei, L.T. Yang, F. Guo, S.B. Tao, L. Cheng, R.S. Huang, L. Ma, P. Fu. Activation of GPR120 in podocytes ameliorates kidney fibrosis and inflammation in diabetic nephropathy. ***Acta pharmacologica Sinica***. 2021, 42: 252-263. https://doi.org/10.1038/s41401-020-00520-4

15. S. Tao, L. Yang, C. Wu, Y. Hu, F. Guo, Q. Ren, L. Ma, P. Fu. Gambogenic acid alleviates kidney fibrosis via epigenetic inhibition of EZH2 to regulate Smad7-dependent mechanism. ***Phytomedicine : international journal of phytotherapy and phytopharmacology***. 2022, 106: 154390. https://doi.org/10.1016/j.phymed.2022.154390

16. B. Wang, J. Xu, Q. Ren, L. Cheng, F. Guo, Y. Liang, L. Yang, Z. Tan, P. Fu, L. Ma. Fatty acid-binding protein 4 is a therapeutic target for septic acute kidney injury by regulating inflammatory response and cell apoptosis. ***Cell death & disease***. 2022,

13: 333. https://doi.org/10.1038/s41419-022-04794-w

17. A.D. Pradhan, J.E. Manson, N. Rifai, J.E. Buring, P.M. Ridker. C-reactive protein, interleukin 6, and risk of developing type 2 diabetes mellitus. ***Jama***. 2001, 286: 327-334. https://doi.org/10.1001/jama.286.3.327

18. L. Wu, C. Liu, D.Y. Chang, R. Zhan, J. Sun, S.H. Cui, S. Eddy, V. Nair, E. Tanner, F.C. Brosius, H.C. Looker, R.G. Nelson, M. Kretzler, J.C. Wang, M. Xu, W. Ju, M.H. Zhao, M. Chen, L. Zheng. Annexin A1 alleviates kidney injury by promoting the resolution of inflammation in diabetic nephropathy. ***Kidney international***. 2021, 100: 107-121. https://doi.org/10.1016/j.kint.2021.02.025

19. C.A. Ricciardi, L. Gnudi. Kidney disease in diabetes: From mechanisms to clinical presentation and treatment strategies. ***Metabolism: clinical and experimental***. 2021, 124: 154890. https://doi.org/10.1016/j.metabol.2021.154890

20. K. Susztak, A.C. Raff, M. Schiffer, E.P. Böttinger. Glucose-induced reactive oxygen species cause apoptosis of podocytes and podocyte depletion at the onset of diabetic nephropathy. ***Diabetes***. 2006, 55: 225-233.

21. D. Yang, M.J. Livingston, Z. Liu, G. Dong, M. Zhang, J.K. Chen, Z. Dong. Autophagy in diabetic kidney disease: regulation, pathological role and therapeutic potential. ***Cellular and molecular life sciences : CMLS***. 2018, 75: 669-688. https://doi.org/10.1007/s00018-017-2639-1

22. F. Jin, X. Li, Y. Deng, M. Timilshina, B. Huang, D.Y. Kim, J.H. Chang, H. Ichinose, S.H. Baek, M. Murakami, Y.J. Lee, H.W. Chang. The orphan nuclear receptor NR4A1 promotes FcεRI-stimulated mast cell activation and anaphylaxis by counteracting the inhibitory LKB1/AMPK axis. ***Allergy***. 2019, 74: 1145-1156. https://doi.org/10.1111/all.13702

23. Y.Y. Zhan, Y. Chen, Q. Zhang, J.J. Zhuang, M. Tian, H.Z. Chen, L.R. Zhang, H.K. Zhang, J.P. He, W.J. Wang, R. Wu, Y. Wang, C. Shi, K. Yang, A.Z. Li, Y.Z. Xin, T.Y. Li, J.Y. Yang, Z.H. Zheng, C.D. Yu, S.C. Lin, C. Chang, P.Q. Huang, T. Lin, Q. Wu. The orphan nuclear receptor Nur77 regulates LKB1 localization and activates AMPK. ***Nature chemical biology***. 2012, 8: 897-904.

https://doi.org/10.1038/nchembio.1069

24. K. Zhu, Z. Meng, Y. Tian, R. Gu, Z. Xu, H. Fang, W. Liu, W. Huang, G. Ding, W. Xiao. Hypoglycemic and hypolipidemic effects of total glycosides of Cistanche tubulosa in diet/streptozotocin-induced diabetic rats. ***Journal of ethnopharmacology***. 2021, 276: 113991. https://doi.org/10.1016/j.jep.2021.113991

25. A. Galli, P. Marciani, A. Marku, S. Ghislanzoni, F. Bertuzzi, R. Rossi, A. Di Giancamillo, M. Castagna, C. Perego. Verbascoside Protects Pancreatic β-Cells against ER-Stress. ***Biomedicines***. 2020, 8. https://doi.org/10.3390/biomedicines8120582

26. W. Gong, N. Zhang, G. Cheng, Q. Zhang, Y. He, Y. Shen, Q. Zhang, B. Zhu, Q. Zhang, L. Qin. Rehmannia glutinosa Libosch Extracts Prevent Bone Loss and Architectural Deterioration and Enhance Osteoblastic Bone Formation by Regulating the IGF-1/PI3K/mTOR Pathway in Streptozotocin-Induced Diabetic Rats. ***International journal of molecular sciences***. 2019, 20. https://doi.org/10.3390/ijms20163964

27. M.A. Pearen, G.E. Muscat. Minireview: Nuclear hormone receptor 4A signaling: implications for metabolic disease. ***Molecular endocrinology (Baltimore, Md.)***. 2010, 24: 1891-1903. https://doi.org/10.1210/me.2010-0015

28. J.C. Helbling, A.M. Minni, V. Pallet, M.P. Moisan. Stress and glucocorticoid regulation of NR4A genes in mice. ***Journal of neuroscience research***. 2014, 92: 825-834. https://doi.org/10.1002/jnr.23366

29. K. Duszka, J.G. Bogner-Strauss, H. Hackl, D. Rieder, C. Neuhold, A. Prokesch, Z. Trajanoski, A.M. Krogsdam. Nr4a1 is required for fasting-induced down-regulation of Pparγ2 in white adipose tissue. ***Molecular endocrinology (Baltimore, Md.)***. 2013, 27: 135-149. https://doi.org/10.1210/me.2012-1248

30. C. Mazuy, M. Ploton, J. Eeckhoute, W. Berrabah, B. Staels, P. Lefebvre, A. Helleboid-Chapman. Palmitate increases Nur77 expression by modulating ZBP89 and Sp1 binding to the Nur77 proximal promoter in pancreatic β-cells. ***FEBS letters***. 2013. https://doi.org/10.1016/j.febslet.2013.10.024

31. L. Pei, A. Castrillo, P. Tontonoz. Regulation of macrophage inflammatory gene expression by the orphan nuclear receptor Nur77. ***Molecular endocrinology (Baltimore, Md.)***. 2006, 20: 786-794. https://doi.org/10.1210/me.2005-0331

32. D. Zhong, Z. Wan, J. Cai, L. Quan, R. Zhang, T. Teng, H. Gao, C. Fan, M. Wang, D. Guo, H. Zhang, Z. Jia, Y. Sun. mPGES-2 blockade antagonizes β-cell senescence to ameliorate diabetes by acting on NR4A1. ***Nature metabolism***. 2022, 4: 269-283. https://doi.org/10.1038/s42255-022-00536-6

33. L. Zhang, Q. Wang, W. Liu, F. Liu, A. Ji, Y. Li. The Orphan Nuclear Receptor 4A1: A Potential New Therapeutic Target for Metabolic Diseases. ***Journal of diabetes research***. 2018, 2018: 9363461. https://doi.org/10.1155/2018/9363461

34. L. Pei, H. Waki, B. Vaitheesvaran, D.C. Wilpitz, I.J. Kurland, P. Tontonoz. NR4A orphan nuclear receptors are transcriptional regulators of hepatic glucose metabolism. ***Nature medicine***. 2006, 12: 1048-1055. https://doi.org/10.1038/nm1471

35. M. Berriel Diaz, U. Lemke, S. Herzig. Discovering orphans' sweet secret: NR4A receptors and hepatic glucose production. ***Cell metabolism***. 2006, 4: 339-340. https://doi.org/10.1016/j.cmet.2006.10.005

36. Y. Zhan, X. Du, H. Chen, J. Liu, B. Zhao, D. Huang, G. Li, Q. Xu, M. Zhang, B.C. Weimer, D. Chen, Z. Cheng, L. Zhang, Q. Li, S. Li, Z. Zheng, S. Song, Y. Huang, Z. Ye, W. Su, S.C. Lin, Y. Shen, Q. Wu. Cytosporone B is an agonist for nuclear orphan receptor Nur77. ***Nature chemical biology***. 2008, 4: 548-556. https://doi.org/10.1038/nchembio.106

37. X.M. Li, X.X. Lu, Q. Xu, J.R. Wang, S. Zhang, P.D. Guo, J.M. Li, H. Wu. Nur77 deficiency leads to systemic inflammation in elderly mice. ***Journal of inflammation (London, England)***. 2015, 12: 40. https://doi.org/10.1186/s12950-015-0085-0

38. A.A. Hamers, L. van Dam, J.M. Teixeira Duarte, M. Vos, G. Marinković, C.M. van Tiel, S.L. Meijer, A.M. van Stalborch, S. Huveneers, A.A. Te Velde, W.J. de Jonge, C.J. de Vries. Deficiency of Nuclear Receptor Nur77 Aggravates Mouse Experimental Colitis by Increased NFκB Activity in Macrophages. ***PloS one***. 2015, 10: e0133598. https://doi.org/10.1371/journal.pone.0133598

DOI: 10.55415/deep-2023-0011.v1

39. R.N. Hanna, I. Shaked, H.G. Hubbeling, J.A. Punt, R. Wu, E. Herrley, C. Zaugg, H. Pei, F. Geissmann, K. Ley, C.C. Hedrick. NR4A1 (Nur77) deletion polarizes macrophages toward an inflammatory phenotype and increases atherosclerosis. ***Circulation research***. 2012, 110: 416-427. https://doi.org/10.1161/circresaha.111.253377